Proceedings of ICRC 2001: 3661 © Copernicus Gesellschaft 2001

ICRC 2001

# The antiproton to proton ratio over a 22-year cycle: A time dependent approach

**R. A. Burger**[1], **S. E. S. Ferreira**[1], **J. W. Bieber**[2], **R. Engel**[2], **T. K. Gaisser**[2], **and T. Stanev**[2]

[1]Unit for Space Physics, School of Physics, Potchefstroom University for CHE, 2520 Potchefstroom, South Africa
[2]Bartol Research Institute, University of Delaware, Newark DE 19716, United States of America

**Abstract.** The prediction from a steady-state two-dimensional numerical modulation model is that the antiproton to proton ratio should exhibit a "w" shape during $A > 0$ solar polarity cycles, and an "M" shape during $A < 0$ cycles. Moreover, the ratio should show smaller variations during an $A > 0$ cycle than during an $A < 0$ cycle and a sharp increase going through solar maximum from one cycle to the other. In this paper we present results from both a two-dimensional time-dependent numerical modulation model and a steady-state model using the latest interstellar antiproton and proton spectra. The variations in the magnitude of the heliospheric magnetic field and the tilt angle of the heliospheric current sheet are based on smoothed data, but are constructed to give an idealized 22-year cycle with identical variations during each polarity cycle. Qualitative conclusions based on a steady-state model's results remain valid, but the ratio now behaves differently during periods of increasing and decreasing solar activity. We find better qualitative agreement with data with this more realistic approach.

## 1 Introduction

In previous papers (Bieber et al., 1999a,b) we discussed the modulation of protons and antiprotons based on the results of a steady-state two-dimensional numerical modulation code (Burger and Hattingh, 1995). Given the simplicity of the model we found surprisingly good agreement with typical data for the ratio of oppositely charged particles over a 22-year solar polarity cycle. Our models showed a small variation in the ratio during an $A > 0$ cycle, a rapid increase going from one polarity cycle to the other and larger variations in the ratio during an $A < 0$ cycle. We now use a time-dependent two-dimensional modulation code for our calculations (le Roux and Potgieter, 1990) and more realistic variations in the tilt angle of the heliospheric current sheet, the heliospheric magnetic field (HMF) and the magnitude of the solar wind speed during the course of a 22-year cycle. Our main aim is to show how the results from a time-dependent code differ from those of a steady-state code with exactly the same transport coefficients. We also give a brief discussion on work in progress on the calculation of the local interstellar antiproton spectrum.

*Correspondence to:* R.A. Burger (fskrab@puknet.puk.ac.za)

## 2 Modulation model

The cosmic-ray transport equation (TPE) of Parker (1965) can be written in terms of the omnidirectional distribution function $f(\mathbf{r}, p)$ (related to the differential intensity by $j_T \propto p^2 f$) as

$$\nabla \cdot (\mathsf{K}^s \cdot \nabla f) - (\mathbf{v}_d + \mathbf{V}) \cdot \nabla f + \frac{1}{3} (\nabla \cdot \mathbf{V}) \frac{\partial f}{\partial \ln p} = 0. \quad (1)$$

Here $\mathbf{r}$ is position, $p$ is momentum, $\mathsf{K}^s$ is the symmetric part of the diffusion tensor, $\mathbf{V}$ is the solar wind velocity, and $\mathbf{v}_d = \frac{pv}{3q} \nabla \times \frac{\mathbf{B}}{B^2}$ the particle drift velocity for a near-isotropic particle distribution due to the curvature and gradient of the HMF, with $v$ and $q$ respectively particle speed and signed charge, and $\mathbf{B}$ the heliospheric magnetic field (Jokipii and Kóta, 1989).

For diffusion parallel to the mean magnetic field we use the result of le Roux et al. (1999),

$$\kappa_{||} = 0.811 v \frac{r_g^{1/3} l_b^{2/3}}{A_B^2} \left[ 0.0972 \left( \frac{r_g}{l_b} \right)^{5/3} + 1 \right]. \quad (2)$$

Here $r_g$ is the particle gyroradius, $l_b$ is the wavelength for slab turbulence at the point separating the energy and the inertial range in the power spectrum of slab HMF fluctuations, and $A_B$ is the normalized amplitude of the $x$ component of the slab HMF fluctuations. Our aim is not to fit data and therefore we simply assume that $A_B$ is constant and that $l_b$ scales as $r^{-1/3}$. For diffusion perpendicular to the mean magnetic field we use $\kappa_\perp^{r\phi} = a\kappa_{||}$ and $\kappa_{\theta\theta} = b(\theta)\kappa_{||}$ with $a$ constant and $b(\theta)$ a function that increases from the ecliptic region to the polar region. We further assume that $\kappa_{||}$ is

smaller during $A > 0$ cycles than during $A < 0$ cycles, and use the weak-scattering limit for the drift coefficient. For some runs drifts were scaled down once the tilt angle was above $75^\circ$ so that the drift coefficient was zero when the tilt angle was $90^\circ$. This modification turned out to have very little effect on our solutions. Note that in Burger et al. (2001) drift effects in other models of the HMF, including the model of Fisk (1996) and also during solar maximum conditions, are estimated. During solar minimum conditions we assume that the solar wind has a speed of 400 km/s in the ecliptic region and 800 km/s in the polar regions. This is assumed to change with increasing solar activity until the speed is a uniform 600 km/s during solar maximum conditions. For the time-dependence of the magnitude of the HMF and the tilt angle of the heliospheric current sheet we use models based on smoothed data. These models are constructed in such a way that we obtain smooth, idealized 11-year cycles. They are discussed below.

## 3 Calculation of interstellar antiproton spectrum

Under the assumption of a thin galactic disk surrounded by a flat halo with a thickness much larger than that of the disk, the diffusion equation for galactic cosmic ray transport is to a large extent equivalent to a simple leaky box model. The modified weighted slab technique can be used to perform the reduction of the diffusion equation to a leaky box expression (for example, Jones et al. (2001) and references therein). It also links the diffusion model parameters to the escape length parameter of the leaky box model. Using this technique, Jones et al. (2001) investigated predictions of various galactic propagation models on primary to secondary particle ratios such as on B/C and sub-Fe/Fe. In the following we apply the results of Jones et al. (2001) to the calculation of the interstellar antiproton spectrum. We repeat our calculation of Bieber et al. (1999a) for two of the models considered in Jones et al. (2001), the disk-halo diffusion model and the turbulent diffusion model.

Neglecting ionization losses, the continuity equation for secondary antiproton production (Gaisser and Schaefer, 1992) is written as

$$\frac{1}{\lambda_e} J_{\bar{p}}(E_{\bar{p}}) + \frac{1}{\lambda_i} J_{\bar{p}}(E_{\bar{p}}) = \frac{c}{4\pi \langle m \rangle} Q(E_{\bar{p}}; J_{\bar{p}}(E_{\bar{p}})), \qquad (3)$$

where $\lambda_e$ is the characteristic escape length, $J_{\bar{p}}(E_{\bar{p}})$ denotes the antiproton flux, and $\lambda_i$ is the interaction length for inelastic collisions of antiprotons with the interstellar gas (annihilation and non-annihilation contributions). The average mass of the particles of the interstellar medium is $\langle m \rangle = \sum_j n_j m_j / \sum_j n_j$, with $n_j$ being the interstellar number density of particles of type $j$.

The antiproton source term $Q$ receives contributions from antiproton production in cosmic ray interactions with the interstellar gas

$$Q_{\bar{p}}(E_{\bar{p}}) = \frac{4\pi}{c} \sum_{i,j} n_j \int_{E_{\rm th}}^{\infty} \frac{2\, d\sigma_{i,j\to\bar{p}}}{dE_{\bar{p}}} J_i(E_i) dE_i \,, \qquad (4)$$

and high-energy antiprotons which lose energy in inelastic scattering processes

$$Q_{\rm scatt}(E_{\bar{p}}) = \frac{4\pi}{c} \sum_j n_j \int_{E_{\bar{p}}}^{\infty} \left\{ \frac{d\sigma_{\bar{p},j\to\bar{p}}}{dE_{\bar{p}}} + \frac{d\sigma_{\bar{p},j\to\bar{n}}}{dE_{\bar{n}}} \right\} \cdot J_{\bar{p}}(E) dE \,. \qquad (5)$$

The index $i$ sums over primary cosmic ray particles and $j$ runs over all interstellar gas target particle species (H, He, CNO). Details of the calculation can be found in Bieber et al. (1999a) and Gaisser et al. (1999).

The only parameter of the leaky box model directly related to cosmic ray transport is the escape length. It reflects assumptions on the galactic disk and halo structure as well as considered transport processes. In a disk-halo diffusion model the data on secondary to primary ratios can be well described using the parameterization

$$\lambda_e = \begin{cases} X_0 \beta & : R < R_0 \\ X_0 \beta (R/R_0)^{-a} & : R \geq R_0 \end{cases} \qquad (6)$$

with $X_0 = 11.8$ g/cm$^2$, $R_0 = 4.9$ GV, and $a = 0.54$ (Jones et al., 2001). The result of the turbulent diffusion model can be represented as

$$\lambda_e = \frac{\beta X_0}{1 + \beta (R/R_0)^a}. \qquad (7)$$

Again we use the parameters as given in Jones et al. (2001): $X_0 = 14.5$ g/cm$^2$, $R_0 = 15$ GV, and $a = 0.85$. Both models predict antiproton fluxes which are very similar to our previous result (Bieber et al., 1999a), as shown in Figure 1. For the purposes of the present paper we will therefore use the results of Bieber et al. (1999a).

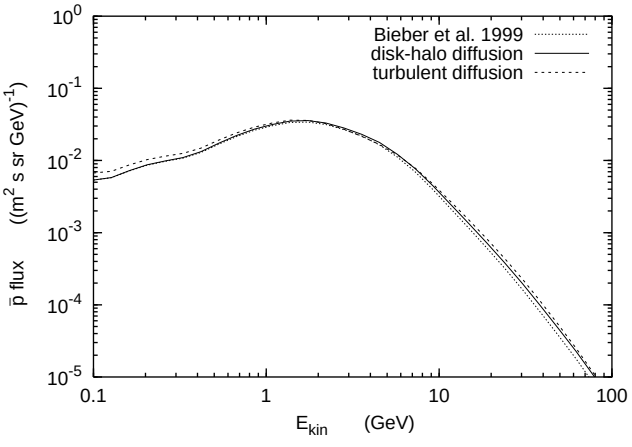


**Fig. 1.** Comparison of interstellar antiproton fluxes.

## 4 Model results

The bottom panel of Figure 2 shows the models for the tilt angle and the magnitude of the HMF used in our code. The tilt angle is allowed to reach $90^\circ$ at which point the magnetic field polarity is switched. The possible importance of the

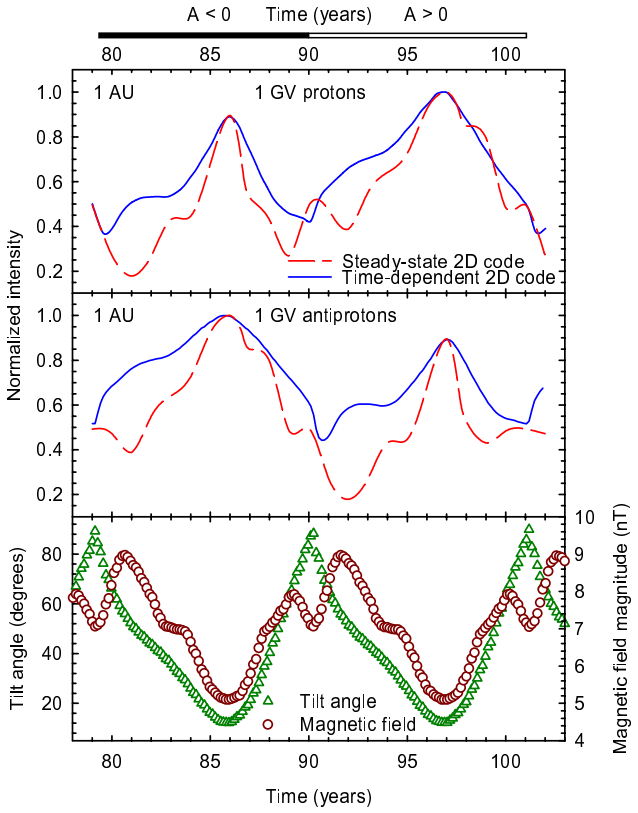


**Fig. 2.** *Top panels*: The intensity-time profile for 1 GV protons and antiprotons from the time-dependent model (solid lines) and the steady-state model (dashed lines). *Bottom panel*: The heliospheric tilt angle (triangles; left axis) and the HMF magnitude (circles; right axis) used in the models.

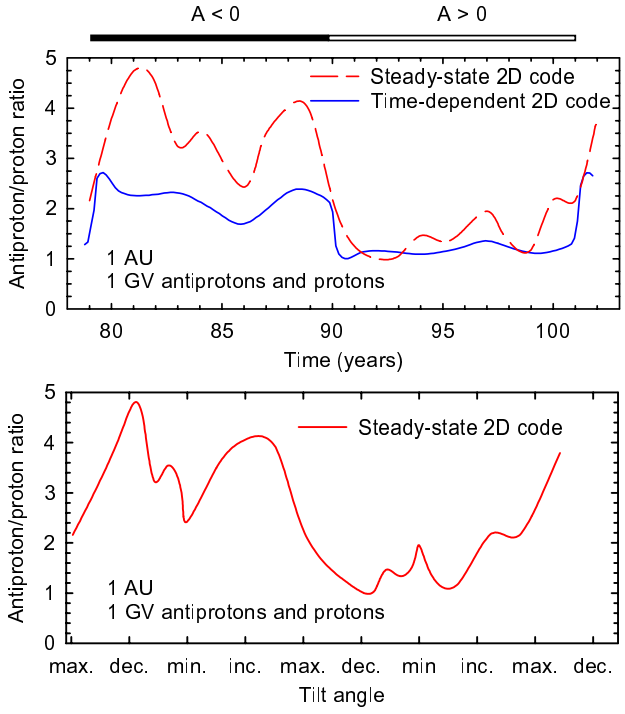


**Fig. 3.** *Top panel*: Ratio of 1 GV antiprotons to protons from the time-dependent model (solid lines) and the steady-state model (dashed lines) as function of time. *Bottom panel*: Ratio of 1 GV antiprotons to protons from the steady-state model as function of tilt angle.

current sheet when the tilt angle becomes very large has been pointed out previously by Thomas et al. (1986). Note that the years in these figures are not meant to be interpreted as actual dates. The top and the middle panel of Figure 2 show the intensity-time profiles of 1 GV protons and antiprotons at Earth, respectively. In each case the intensity is normalized with respect to the highest value. Solid lines indicate results from the time-dependent two-dimensional code and dashed lines from the steady-state code. In both cases the intensity profile for protons is flatter during an $A > 0$ cycle than during an $A < 0$ cycle; for antiprotons the opposite is true. In the two-dimensional steady-state code changes in the tilt angle and HMF occur simultaneously throughout the heliosphere while they propagate out from the Sun at the solar wind speed in the time-dependent model. It is therefore not surprising that the steady-state solutions react much stronger to such changes than the time-dependent solutions, and show more fine structure. Consider as an example the behaviour of the antiprotons in the period from about year 90 to 92. For both models the intensity decreases through solar maximum, but whereas the intensity for the steady-state model keeps on decreasing, the intensity for the time-dependent model starts to increase. In the latter case the increase in the HMF magnitude after year 90 is offset to a large extend by the previous decrease, the effect of which is still present at larger radial distances. The model therefore reacts more readily to the decrease in tilt angle and consequently the intensity increases. In a short period around solar minimum the models agree, as they should.

Figure 3 shows the antiproton to proton ratio of 1 GV particles at Earth, the top panel for both models as function of time and the bottom panel for the steady-state model only, now as function of tilt angle. In each case the ratio is normalized with respect to its lowest value. Although the ratios in the top panel share qualitative features, the steady-state model shows a much larger increase going from one cycle to the other, but at a somewhat slower rate of change than the time-dependent approach. We have shifted the data from the time-dependent code to earlier times to compensate for the time it takes to establish the new solar magnetic polarity. Because we use smoothed tilt angles and HMF magnitudes we can relate features in these quantities to features in the ratio. Consider for example the local maximum in the ratio for the steady-state results around year 84 of the $A < 0$ cycle. During this period the polar solar wind speed is increasing, which tends to decrease the intensity of the protons drifting in from the solar polar regions to Earth. The antiprotons, drifting in along the current sheet to Earth, are not subject to this decrease, because they are much less affected by a change in solar wind speed in the ecliptic region. The combination of the change in intensity caused by the changing

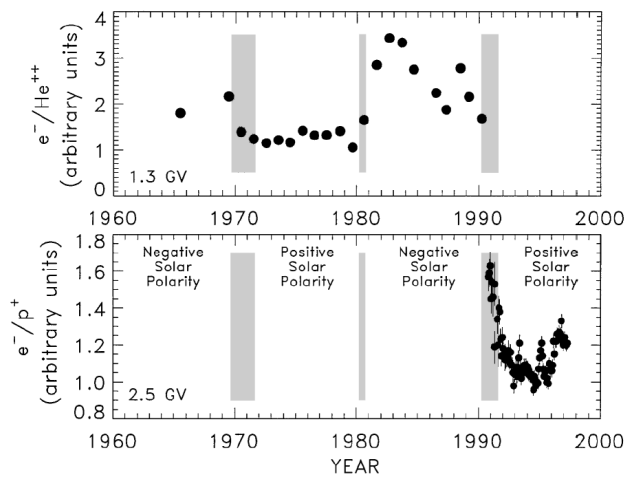


**Fig. 4.** Ratio of (top) electrons to helium at 1.3 GV rigidity and (bottom) electrons to protons at 2.5 GV rigidity. Shaded areas delimit time periods Positive and negative solar polarity refer to epochs when the magnetic field emerging from the Sun's north poles point respectively, outward and inward. From Bieber et al. (1999a).

solar wind speed and the fact that the HMF magnitude becomes almost constant around year 84, is enough to cause a slight decrease in the proton intensity even though the tilt angle is also decreasing, causing an increase in intensity. The antiproton intensity is increasing because of the decrease in tilt angle, and therefore the antiproton to proton ratio shows an increase around year 84. One can then argue that in this case it is the fact that the HMF magnitude remains constant that causes the local maximum in the ratio.

Finally we compare the qualitative features of the observed electron to Helium and electron to proton ratio shown in Figure 4 to those of Figure 3. Both models show some of the same qualitative features as the data. In contrast to our previous results (Bieber et al., 1999a,b) the ratio during an $A < 0$ cycle is not symmetric with respect to solar minimum and the ratio is larger before solar minimum than after.

## 5 Discussion and conclusions

We have shown that the use of more realistic variations in the solar wind speed, the magnitude of the HMF and that of the heliospheric tilt angle, lead to better qualitative agreement of both the time-dependent and the steady-state calculations of the antiproton to proton ratio with data, albeit for different species. The time-dependent model shows less prominent features in the antiproton to proton ratio and gives smaller overall effects than the steady-state model when using the same transport coefficients, HMF, tilt angle and solar wind speed.

For an alternative approach to time- and charge-sign dependent modulation and a direct comparison between models and data see Potgieter and Ferreira (2001).

*Acknowledgements.* RAB and SESF thank Marius Potgieter for many useful discussion. This work was supported by NASA grant NAG5-5181.

## References

Bieber, J. W., Burger R. A., Engel, R., Gaisser, T. K., Roesler, S. and Stanev, T., Antiprotons at solar maximum, Phys. Rev. Lett., 84, 674-677, 1999a.

Bieber, J. W., Burger R. A., Engel, R., Gaisser, T. K. and Stanev, T. 1999. Antiprotons as probes of solar modulation, Proc. 26th Int. Cosmic Ray Conf., 7, 17-20, 1999b.

Burger, R. A. and Hattingh, M., Steady-state drift-dominated modulation models for galactic cosmic rays, Astrophys. Space Sci., 230, 375-382, 1995.

Burger, R. A., Potgieter, M. S. and Heber, B., Rigidity dependence of cosmic-ray proton latitudinal gradients measured by the Ulysses spacecraft: Implications for the diffusion tensor, J. Geophys. Res, 105(A12), 27,447-27,456, 2000.

Burger, R. A., Van Niekerk, Y. and Potgieter, M. S., An estimate of drift effects in various models of the heliospheric magnetic field, Space Sci. Rev., In press, 2001.

Fisk, L. A., Motion of the footpoints of heliospheric magnetic field lines at the Sun: Implications for recurrent energetic particle events at high heliographic latitudes, J. Geophys. Res., 101, 15547-15553, 1996.

Gaisser, T. K., Bieber, J. W., Burger, R. A., Engel, R., Roesler, S. and Stanev, T., Antiprotons in the Galaxy, Proc. of the 26th Int. Cosmic Ray Conf., 3, 69-72 , 1999.

Gaisser, T. K. and Schaefer, R. K., Cosmic-ray secondary antiprotons: a closer look, Astrophys. J., 394, 174-183, 1992.

Jokipii, J. R. and Kóta, J., The polar heliospheric magnetic field, Geophys. Res. Lett., 16, 1-4, 1989.

Jones, F. J., Lukasiak, A., Ptuskin, V. and Webber, W., The modified slab technique: models and results, Astrophys. J., 547, 264-271, 2001.

le Roux, J. A. and Potgieter, M. S., A time-dependent drift model for the long-term modulation of cosmic rays with special reference to asymmetries with respect to the solar minimum of 1987, Astrophys. J., 361, 275-282, 1990.

le Roux, J. A., Zank, G. P. and Ptuskin, V. S., An evaluation of perpendicular diffusion models regarding cosmic ray modulation on the basis of a hydromagnetic description for solar wind turbulence, J. Geophys. Res., 104, 24,845-24,862, 1999.

Parker, E. N., The passage of energetic charged particles through interplanetary space, Planet. Space Sci., 13, 9-49, 1965.

Potgieter, M. S. and Ferreira, S. E. S., A new cosmic ray modulation model for the 11-year and 22-year cycles, SH 3.1, this volume, 2001

Thomas, B. T., Goldstein, B. E. and Smith, E. J. The effect of the heliospheric current sheet on cosmic ray intensities at solar maximum: two alternative hypotheses, J. Geophys. Res. 91, 2889-2895, 1986